


 Cite this: *RSC Adv.*, 2022, **12**, 26686

Pd/Cu-catalyzed access to novel 3-(benzofuran-2-ylmethyl) substituted (pyrazolo/benzo)triazinone derivatives: their *in silico/in vitro* evaluation as inhibitors of chorismate mutase (CM)†

Gangireddy Sujeewan Reddy,^{ab} Sharda Shukla,^{ab} Harshavardhan Bhuktar,^{ab} Kazi Amirul Hossain,^a Rebecca Kristina Edwin,^a Varadaraj Bhat Giliyaru,^b Parimal Misra^a and Manojit Pal  ^{a*}

In view of the reported chorismate mutase (CM or *Mtb*CM) inhibitory activities of 3-indolylmethyl substituted (pyrazolo/benzo)triazinone derivatives the structurally similar 3-(benzofuran-2-ylmethyl) substituted (pyrazolo/benzo)triazinones were designed and evaluated *in silico* against CM. The docking of target molecules was performed at the interface site of *Mtb*CM (PDB: 2FP2). All the best ranked molecules participated in a strong H-bonding with the ILE67 of the B chain at the backbone position in addition to several hydrophobic/van der Waals interactions with the hydrophobic residues. Based on encouraging docking results, the one-pot synthesis of newly designed benzofuran derivatives was carried out using tandem Pd/Cu-catalyzed Sonogashira cross-coupling followed by intramolecular cyclization of 2-iodophenols with appropriate terminal alkynes. A range of novel 3-(benzofuran-2-ylmethyl) substituted (pyrazolo/benzo)triazinone derivatives were prepared in high (>80%) yields. Three molecules *i.e.* **3h**, **3i** and **3m** that participated in good interaction with CM *in silico* showed encouraging (64–65%) inhibition at 30 μ M *in vitro*. An SAR within this class of molecules suggested that the benzotriazinone series in general was better than the pyrazolotriazinone series. Based on molecular docking *in silico*, CM inhibition *in vitro* and computational ADME prediction the benzofuran derivatives **3i** and **3m** seemed to be of further medicinal interest in the context of discovery and development of new anti-tubercular agents.

Received 22nd August 2022
 Accepted 12th September 2022

DOI: 10.1039/d2ra05255e
rsc.li/rsc-advances

1. Introduction

While COVID-19 has emerged as the leading cause of death worldwide since 2019, tuberculosis (TB) the previous major killer still poses a considerable threat to human health. Indeed, as a single infectious agent *Mycobacterium tuberculosis* has been the cause of death of 1.4 million people including 0.2 million HIV-positive patients according to the 2020 report of the WHO.¹ Besides the co-morbidity with HIV-AIDS the other factors causing TB related death include the long treatment duration *e.g.* 6–9 months, increased occurrence of multi or extensive drug resistance and declining importance or endeavor in anti-infective drug research. Over the years chorismate mutase or CM (EC 5.4.99.5) or *Mtb*CM (*Mycobacterium tuberculosis* CM) has been explored as one of the pharmacological targets for the

identification of potential anti-tubercular agents.² Because of its presence in bacteria but not in animals and its key role in the survival of bacteria^{2–4} the enzyme CM (that catalyzes the Claisen rearrangement of chorismate to prephenate) has emerged as an interesting drug target. Due to our interest in the area of anti-tubercular agents⁵ we have reported the synthesis and evaluation of a range of small organic molecules as inhibitors of CM.^{6,7} Recently, we have explored the 3-indolylmethyl substituted (pyrazolo/benzo)triazinone derivatives **A** (Fig. 1) for the identification of potent inhibitors of CM.⁸ In further continuation of this research we became interested in assessing a library of compounds represented by **B** (Fig. 1) that was obtained *via* replacing the indole moiety of **A** by a benzofuran ring. The choice of benzofuran framework was mainly prompted by the fact that beside being an integral part of several reagents such as benz bromarone, amiodarone, *etc.* (that are already in patient use) this framework has been explored previously for the identification of anti-tubercular as well as anti-bacterial agents.⁹ Further, chemically both indole and the benzofuran ring share some common structural features.

Moreover, CM inhibitory potential of benzofuran derivatives have been documented recently.¹⁰ Herein, we report the *in silico*

^aDr. Reddy's Institute of Life Sciences, University of Hyderabad Campus, Gachibowli, Hyderabad 500 046, India. E-mail: manojitpal@rediffmail.com

^bManipal College of Pharmaceutical Sciences, Manipal Academy of Higher Education, Madhav Nagar, Manipal 576 104, Karnataka, India

† Electronic supplementary information (ESI) available: Experimental procedures and spectral data (file type: word). Copies of spectra of all target compounds synthesized. See <https://doi.org/10.1039/d2ra05255e>



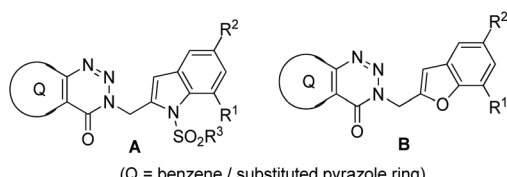


Fig. 1 Reported inhibitors of CM based on (pyrazolo/benzo)triazinone derivatives **A** and the proposed template **B**.

studies, chemical synthesis and *in vitro* CM inhibitory potential of a series compounds based on **B** (Fig. 1).

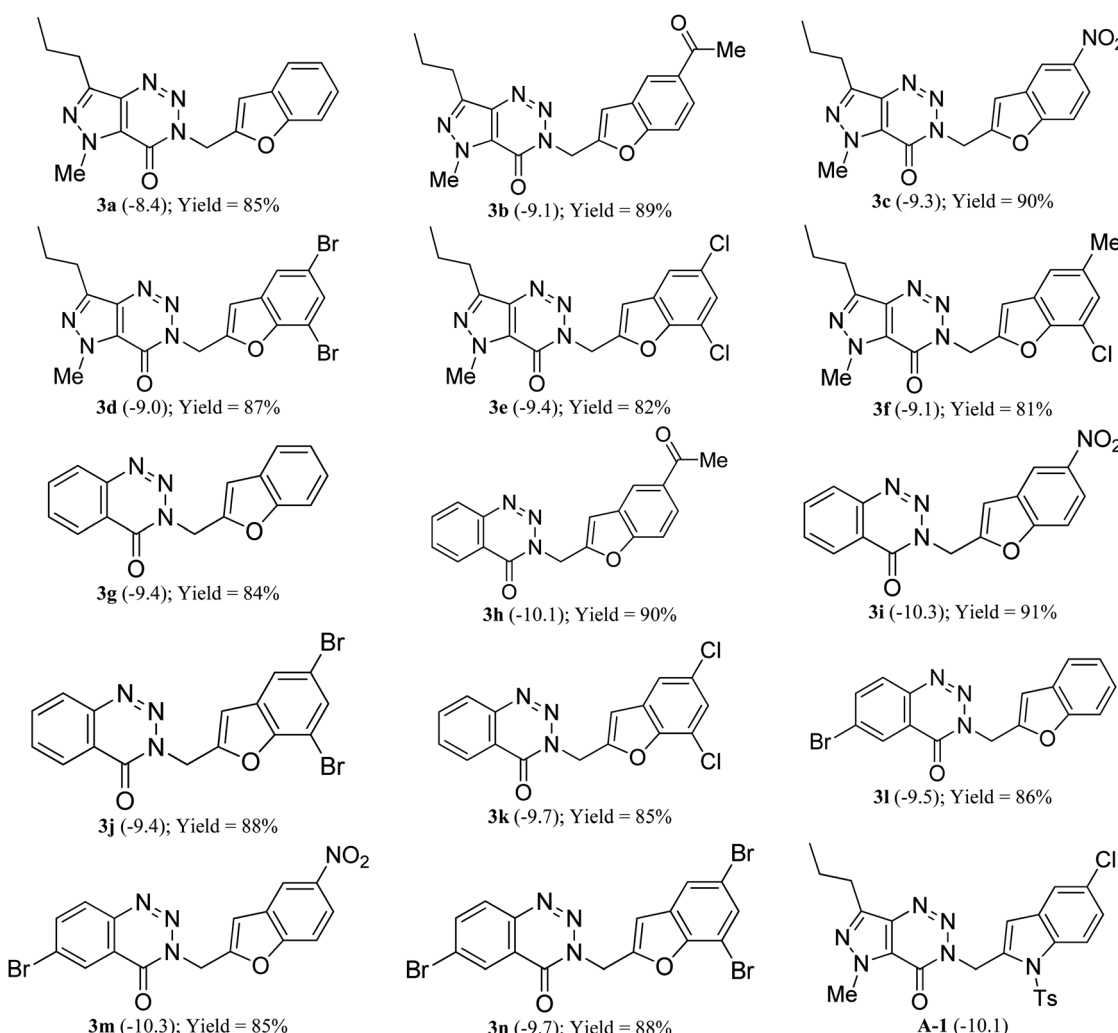
2. Results and discussion

Initially, before undertaking the actual synthesis of library of molecules based on **B** (Fig. 1) the merit and potential of the current designing approach was assessed *via* the *in silico*

docking study of several 3-(benzofuran-2-ylmethyl) substituted (pyrazolo/benzo)triazinone derivatives derived from **B**. Due to the beneficial role of allosteric regulation of protein in its function as well as in many biological processes, the allosteric sites are considered as attractive targets for the design of new NCEs (new chemical entities). On the other hand, study has confirmed the allosteric behavior of *Saccharomyces cerevisiae* chorismate mutase (*ScCM*) on the basis of conformational dynamics and solvent entropy.¹¹ Further, the allosteric inhibition of *MtbCM* by all three aromatic amino acids (Trp, Phe or Tyr at 0.5 mM) at interface site has been noted previously.¹²

Since the binding energy of our studied ligands at interface site was lower than the other possible sites of *MtbCM*, hence we thought that our molecules were preferably stabilized at the interface site of *MtbCM* (which is a homodimer). Nevertheless, the docking of our molecules at the interface site of *MtbCM* (PDB: 2FP2) was performed using the open-source tool AutoDock Vina.¹³ Additionally, the MarvinSketch¹⁴ and AutoDock

Table 1 AutoDock Vina score (kcal mol⁻¹) of compounds docked into the *MtbCM* and the % yield of each compound synthesized^a



^a Figure within the bracket represents AutoDock Vina score (kcal mol⁻¹).



tool¹⁵ were also used for conducting the docking studies and the docking score of the best pose of each ligand along with that of the reported compound⁸ **A-1** is presented in Table 1. To check the reproducibility of docking results, the docking of each individual ligand was performed at least for five times when the maximum difference in the scores obtained was found to be within the range of ± 0.2 . The validation of docking protocol was carried out by re-docking the co-crystal ligand (TSA) and calculating the RMSD difference between co-crystal one and docked one in PyMOL.¹⁶ The maximum RMSD being 1.713 (<2) clearly confirmed the correctness of the docking protocol employed.

Based on docking scores (Table 1) the compound **3h**, **3i** and **3m** (score ~ -10 kcal mol⁻¹) appeared as potential hits in the *in silico* studies and was comparable to the known compound **A-1**. Indeed, the compound **3h** (Fig. 2) formed a strong H-bond

through the ketone carbonyl group with the ILE67 of B chain at the backbone position. Additionally, the molecule also participated in the hydrophobic/van der Waals interactions with the hydrophobic residues (LEU65, PRO66, TYR110, PHE113, LEU65 of both A and B chain) and hydrophobic regions (polar and charged residues *e.g.* GLU68 of both A and B chain and GLN64, LYS117 of A chain). The compound **3i** (Fig. 3) showed H-bonding interaction through its nitro group with the backbone atom of ILE67 of B chain in addition to a π - π interaction with TYR110 of B chain (which could be the reason of its slightly better docking score than compound **3h**). Similar hydrophobic contacts mainly with LEU56, PRO66, PHE113, GLU68, *etc.* of both the chain were also found in this case. Like compound **3i**, the involvement of nitro group in the H-bond interaction was noted for compound **3m** (Fig. 4) in addition to its participation in the usual hydrophobic interactions.

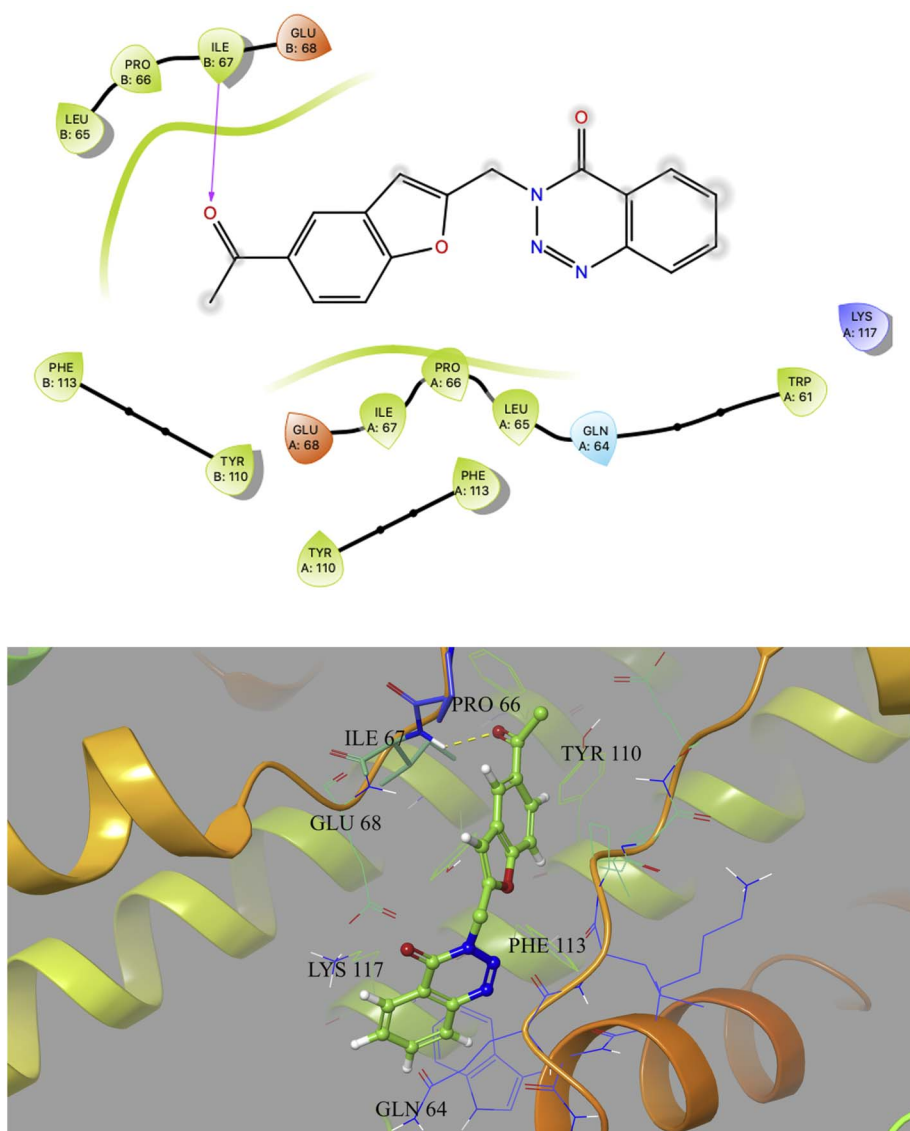


Fig. 2 2D and 3D interaction (H-bond is shown in yellow colour) of compound **3h** with the interface residues of *MtbcM* (PDB: 2FP2) [prepared using Maestro visualizer (Schrödinger, LLC)].



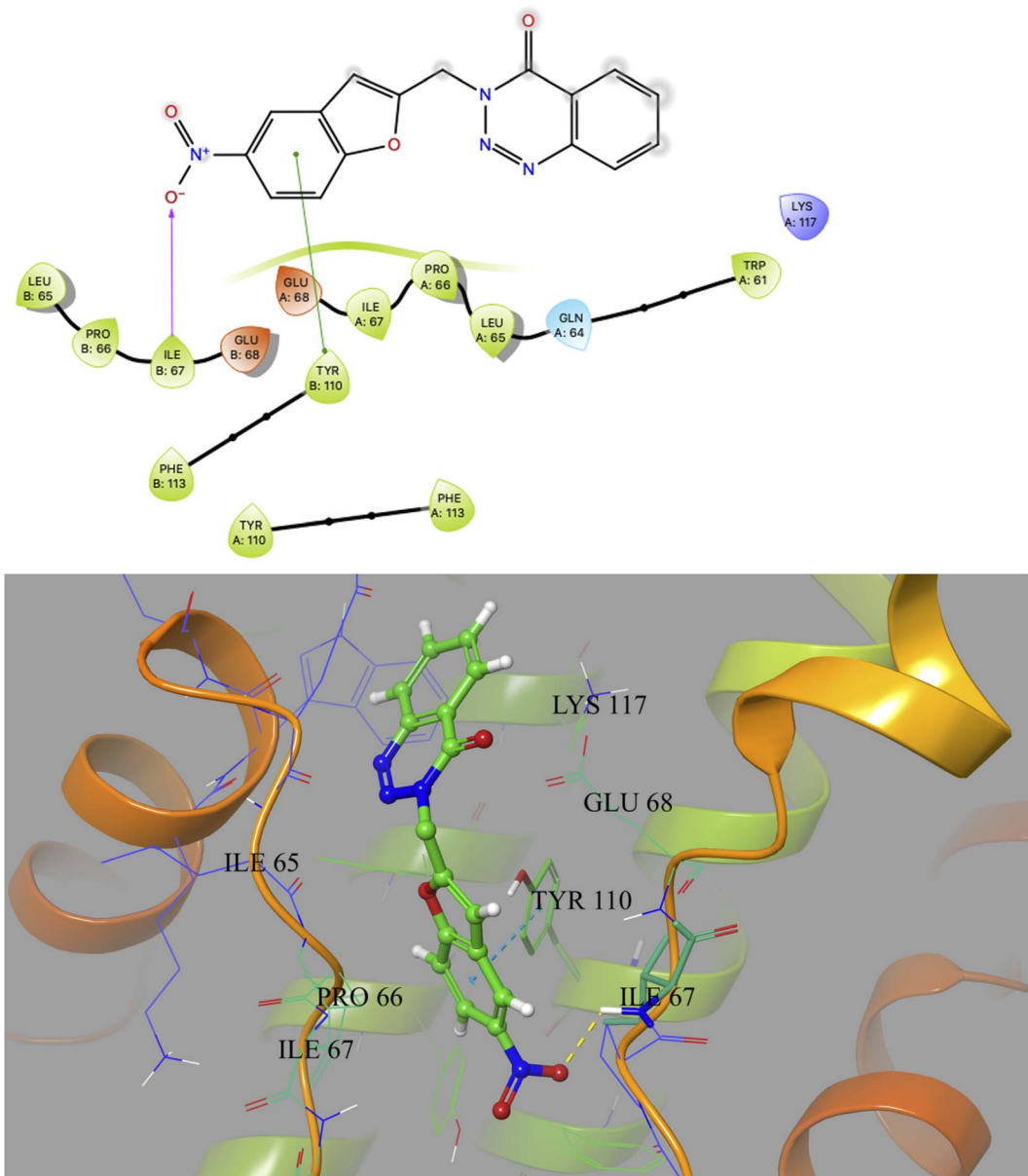


Fig. 3 2D and 3D interaction (H-bond and $\pi-\pi$ interaction shown in yellow and cyan colour, respectively) of compound 3i with the interface residues of MtbCM (PDB: 2FP2).

Nevertheless, in the light of promising overall outcome of the *in silico* study it was become necessary to correlate these observations with the data generated through an *in vitro* assay. Hence, the chemical synthesis as well as some preliminary *in vitro* evaluation of compounds presented in Table 1 was undertaken and the results are presented in the following sections. Notably, the *in silico* studies, synthesis and *in vitro* evaluation of 3-(benzofuran-2-ylmethyl) substituted (pyrazolo/benzo)triazinone derivatives as potential inhibitors of chorismate mutase (CM) was not known previously.

Among the several possible strategies considered for the synthesis of targeted compounds based on **B** (Fig. 1), we envisioned that the construction of the benzofuran ring could be

a convenient as well as effective approach for serving the purpose. While numerous approaches are known for the construction of 2-substituted benzofuran ring,¹⁷ the one-pot method¹⁸⁻³⁵ involving the tandem transition-metal-catalyzed Sonogashira cross-coupling³⁶ followed by intramolecular cyclization of 2-halogenated phenols with terminal alkynes gained considerable interest due to its convenience, functional group tolerance and environmental advantages. Indeed, one of us has been involved in exploring this strategy since 1992 (ref. 37) and its subsequent applications in the preparation of potential bioactive compounds.³⁸⁻⁴¹ In further continuation of this efforts we decided to adopt a similar one-pot synthetic strategy in the current study for accessing the targeted 3-(benzofuran-2-ylmethyl) substituted (pyrazolo/benzo)triazinone derivatives.



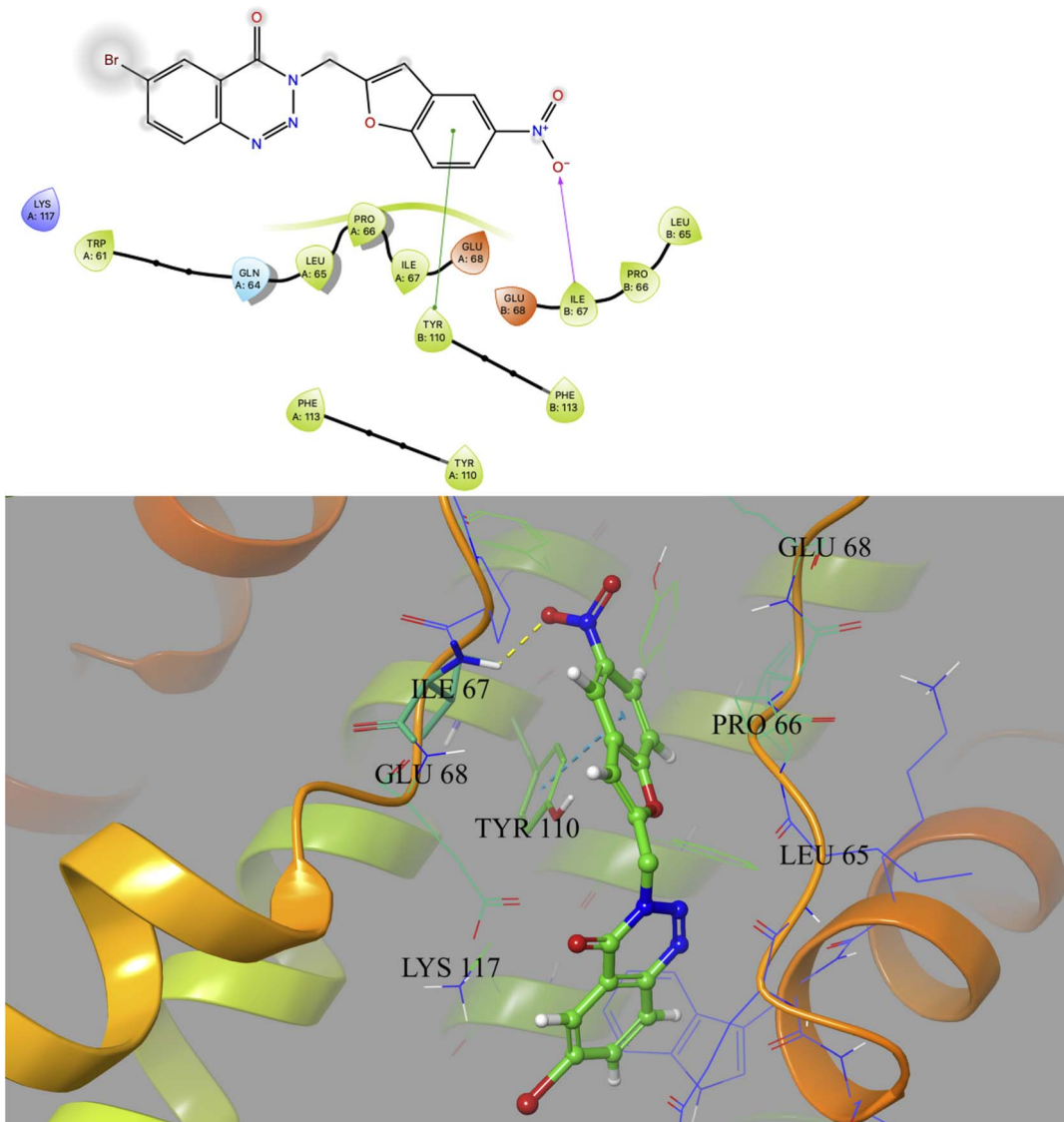
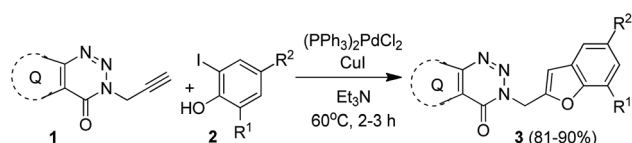


Fig. 4 2D and 3D interaction (H-bond and $\pi-\pi$ interaction shown in yellow and cyan colour, respectively) of compound 3m with the interface residues of MtBCM (PDB: 2FP2).

Thus, the Pd/Cu-catalyzed coupling of the required terminal alkyne (**1**) [e.g. 5-methyl-3-(prop-2-ynyl)-7-propyl-3*H*-pyrazolo [4,3-*d*][1,2,3]triazin-4(5*H*)-one (**1a**) or 3-(prop-2-yn-1-yl)benzo[*d*] [1,2,3]triazin-4(3*H*)-one (**1b**) or 6-bromo-3-(prop-2-yn-1-yl)benzo [*d*][1,2,3]triazin-4(3*H*)-one (**1c**)] obtained *via* the reported method⁸ with appropriate 2-iodophenols (**2**) afforded the expected products (**3**) in good to excellent yields (Scheme 1).

We used a similar reaction conditions reported by us previously^{20,37a} with some suitable modifications as the use of terminal alkyne **1** for the coupling with 2-iodophenols was not explored earlier. For example, a longer reaction time *i.e.* 16–24 h was required in the previously reported method when the reaction was performed using 2–3.5 mol% of $(\text{Ph}_3\text{P})_2\text{PdCl}_2$, 3–5 mol% of CuI and 2 equiv. of Et_3N in DMF. In the current study, we have observed that the reaction time could be decreased significantly with the marginal increase in the catalyst loading such as the use of 5 mol% of $(\text{Ph}_3\text{P})_2\text{PdCl}_2$ and CuI. Nevertheless, a range of reaction conditions by changing the catalyst, base and solvent was examined for the coupling of alkyne **1a** with 2-iodophenol **2a** (Table 1). Among the combination of various Pd-catalyst, ligand PPh_3 and co-catalyst CuI tested (entries 1–7, Table 2), the combination of $(\text{Ph}_3\text{P})_2\text{PdCl}_2$ and CuI (entry 7, Table 2) was found to be most effective for affording the



Scheme 1 Pd/Cu-catalyzed synthesis of 3-(benzofuran-2-ylmethyl) substituted (pyrazolo/benzo)triazinone derivatives.

desired product **3a** in high yield. Further, the use of a solvent such as DMF (entries 1–4, Table 2) or EtOH (entries 5 and 6, Table 2) was counterproductive and was not necessary in the present case because the excess of Et₃N could play the role of base as well as solvent (entry 7, Table 2). Indeed, the reaction was completed within 2 h when performed in Et₃N alone whereas product yield was not increased when longer reaction time was used (entry 7 vs. 8, Table 2). However, in view of the known toxicity of Et₃N an attempt was made to reduce its volume by conducting the reaction using Et₃N as a base, and dry DMF as a solvent in the presence of Pd(PPh₃)₂Cl₂ and CuI as catalysts for 4 h. The desired product **3a** was obtained in 55% yield in this case that was less than that of entry 7 of Table 2. The reaction did not proceed in the absence of co-catalyst CuI (entry 9, Table 2) or the catalyst Pd(PPh₃)₂Cl₂ (entry 10, Table 2). Thus, the condition of entry 7 of Table 2 was used for the preparation of various other analogues of **3a**.

Three different terminal alkynes (**1a–c**) were employed for the reaction with a variety of 2-iodophenols (**2a–f**) in the presence of (Ph₃P)₂PdCl₂ and CuI in Et₃N alone at 60 °C (Table 1). The 2-iodophenols may contain the electron withdrawing group like CH₃CO or NO₂, halogen such as Cl or Br and electron donating group like CH₃. The reactions proceeded smoothly in all these cases and reached to the completion within 2–3 hours affording a range of desired products (**3**) in high (>80%) yields. All the 3-(benzofuran-2-ylmethyl) substituted (pyrazolo/benzo) triazinone derivatives (**3a–n**) obtained were characterized with the help of ¹H as well as ¹³C NMR and MS spectral data. Briefly, the presence of benzofuran ring in these compounds was indicated by the appearance of C-3 proton in ¹H NMR spectra as a singlet in the range δ 6.9–7.2 and C-3 carbon in ¹³C NMR at

106 ppm. The linker “CH₂” moiety appeared near δ 4.5 and 45 ppm in the ¹H and ¹³C NMR spectra, respectively. Further the signal near 155 ppm in ¹³C NMR spectra was due to the “C=O” carbon. These are shown in the selected ¹H and ¹³C NMR data of two representative compounds **3c** and **3i** (Fig. 5). The compound **3c** was further characterized by the presence of NCH₃ group at δ 4.17 and the *n*-propyl protons at δ 2.93 (t, CH₂), 1.86–1.73 (m, CH₂) and 0.94 (t, CH₃) in ¹H NMR spectra.

From the view point of reaction mechanism,^{20,22–24,29,32} the involvement of two key steps *e.g.* Sonogashira coupling followed by intramolecular cyclization in the current approach are depicted in Scheme 2. Thus, the active Pd(0) species generated from Pd(II) participated in oxidative addition to **2** to afford the intermediate **E-1** that on *trans*-organometallation with copper acetylide (generated *in situ* from compound **1** and CuI) followed by reductive elimination of Pd(0) furnished the internal alkyne **E-3** *via* **E-2** thereby completing the first catalytic cycle. In the second catalytic cycle the interaction of Cu(I) species with the alkyne moiety of **E-3** (seemed to be aided by the proximate carbonyl group) formed **E-4** that on intramolecular ring closure afforded **E-5** and then **E-6** and finally the product **3** with the regeneration of CuI to complete the second catalytic cycle.

Next, the CM inhibitory potential of the synthesized compounds **3** was assessed *in vitro*^{42,43} with the help of an assay that measures the catalytic activity of CM during the conversion of substrate chorismate to the product prephenate. The known compound **A-1** (Table 1) and a reported inhibitor⁴⁴ **C** [*i.e.* 4-(3,4-dimethoxyphenethylamino)-3-nitro-5-sulfamoylbenzoic acid] was used as the reference compound in this assay. At the concentration of 30 μM the compound **3h**, **3i** and **3m** showed 63.75 ± 1.09, 65.24 ± 0.98 and 64.90 ± 1.05% inhibition respectively that was comparable to 69.67 ± 0.57% inhibition of the reference compound **A-1** (53.23 ± 0.13% inhibition at 10 μM was observed for the known inhibitor **C**). The other compounds that showed significant inhibition of CM included **3k** (63.66 ±

Table 2 Effect of reaction conditions on coupling of terminal alkyne **1a** with **2a**^a

Entry	Catalyst	Base	Solvent	Time (h)	% Yield ^b
1	10% Pd/C/CuI	K ₂ CO ₃	DMF	6	0 ^c
2	10% Pd/C/PPh ₃ /CuI	K ₂ CO ₃	DMF	6	15 ^d
3	Pd(OAc) ₂ /PPh ₃ /CuI	K ₂ CO ₃	DMF	6	20 ^d
4	Pd(OAc) ₂ /PPh ₃ /CuI	Et ₃ N	DMF	6	30 ^d
5	Pd(OAc) ₂ /PPh ₃ /CuI	Et ₃ N	EtOH	6	20 ^d
6	Pd(PPh ₃) ₂ Cl ₂ /CuI	Et ₃ N	EtOH	6	40 ^c
7	Pd(PPh ₃) ₂ Cl ₂ /CuI	Et ₃ N	Et ₃ N	2	85 ^c
8	Pd(PPh ₃) ₂ Cl ₂ /CuI	Et ₃ N	Et ₃ N	6	83 ^c
9	Pd(PPh ₃) ₂ Cl ₂	Et ₃ N	Et ₃ N	6	0 ^c
10	CuI	Et ₃ N	Et ₃ N	6	0 ^c

^a Reactions were carried out using alkyne **1a** (1 mmol), **2a** (1.2 mmol), catalyst and base (2.0 mmol) in a solvent (5 mL) under nitrogen at 60 °C. ^b Isolated yield. ^c 5 mol% of each catalyst used. ^d 5 mol% of each catalyst and 10 mol% of PPh₃ used.

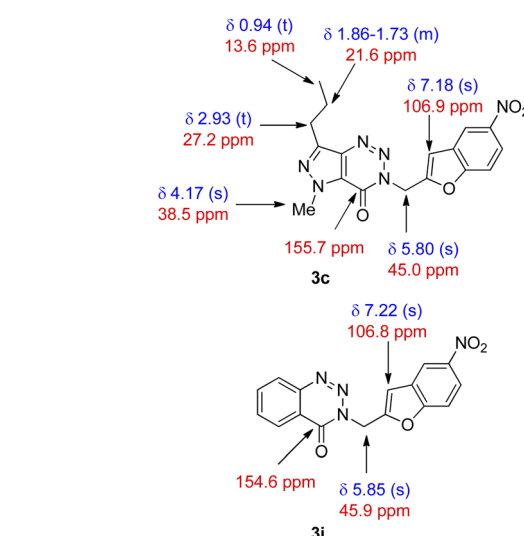
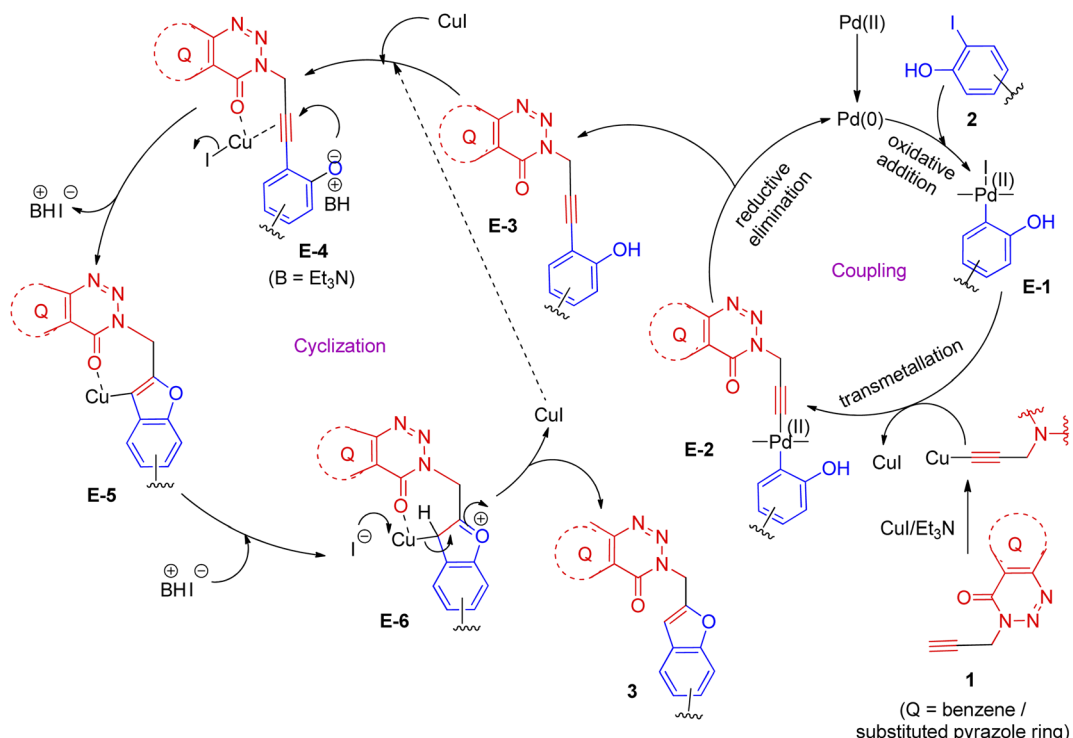


Fig. 5 Selected ¹H (blue) and ¹³C NMR (red) spectral data of compound **3c** and **3i**.





Scheme 2 The plausible reaction mechanism for coupling-cyclization of fused 1,2,3-triazin-4-one based alkyne (1) with o-iodophenols (2) under Pd/Cu-catalysis.

2.07), 3n (63.75 ± 1.12) and 3e (61.28 ± 2.03), 3g (60.27 ± 3.22) and 3j (60.09 ± 2.35). Among rest of the compounds 3a and 3d appeared to be the least active ($>45\%$ inhibition) that was reflected in the results of docking studies. Indeed, the typical H-bonding interaction (as observed in case of active molecules) was missing in case of compound 3a (Fig. 6) due to the lack of any group at C-5 position of its benzofuran ring. Further, though the molecule participated in the hydrophobic interactions but the number of such contacts was lower than that of

active molecules. On the other hand, the compound 3d (Fig. 7) though participated in a H-bond interaction through one of the triazinone nitrogen with the TYR110 of B chain however fewer hydrophobic contacts (with PRO66, ILE67, GLU68 of both A and B chain, and LYS60, TRP61, GLN64, PHE113 of A chain) were noted in this case.

Nevertheless, in general both *in silico* and *in vitro* evaluation suggested that the compounds belonging to the benzotriazinone series emerged as better active molecules than that

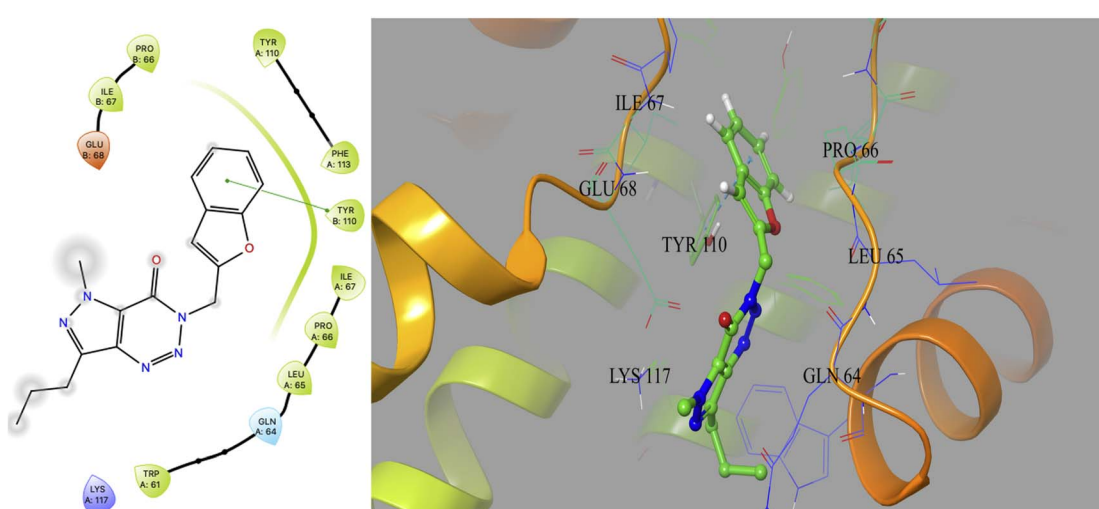


Fig. 6 2D and 3D interaction of compound 3a with the interface residues of MtbcM (PDB: 2FP2).



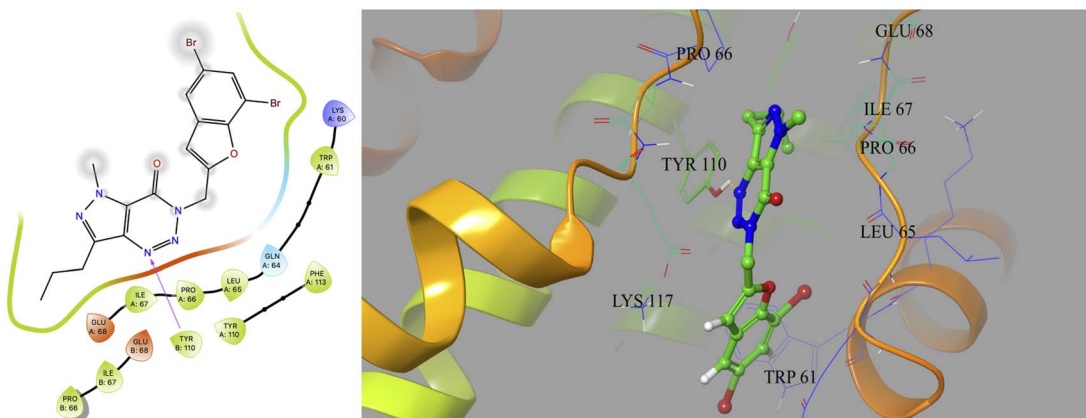


Fig. 7 2D and 3D interaction of compound 3d with the interface residues of MtBCM (PDB: 2FP2).

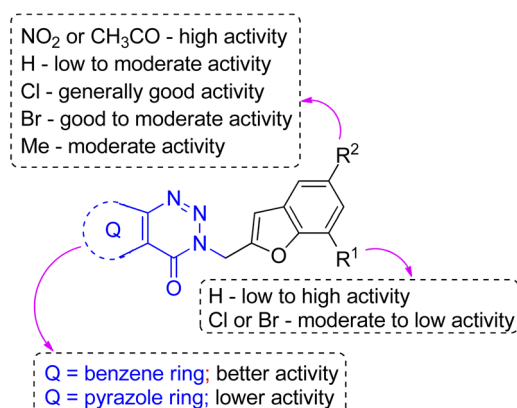


Fig. 8 SAR summary for CM inhibitory activities of compound 3.

from pyrazolotriazinone series. Indeed, all the best active molecules *i.e.* 3h, 3i and 3m emerged from the benzotriazinone series. Thus, an overview of SAR (Structure-Activity-

Relationship) noted for the current series of benzofuran derivatives is presented in Fig. 8. Briefly, the “NO₂” or “CH₃CO” group at C-5 of the benzofuran ring was favorable for CM inhibition while other substituents like Cl, Br or Me or no substituent at this position reduced the activity. A “H” atom at C-7 position was generally better than the “Cl” or “Br” group at the same position in terms of activity. The inhibitory activity was influenced by the aryl/heteroaryl ring fused with the triazinone moiety and as mentioned above, the benzene ring rather than the pyrazole moiety was found to be beneficial for the CM inhibition of the current series of compounds.

In view of usefulness of the early detection of ADME (absorption, distribution, metabolism, and excretion) or pharmacokinetic properties of NCEs the computational ADME prediction of compounds 3h, 3i and 3m along with the reference compound A-1 was carried out using SwissADME webtool.⁴⁵ It is evident from Table 3 that desirable ADME was predicted for compound 3i and 3m with high GI absorption, no BBB (Blood Brain Barrier) penetration and no P-gp substrate

Table 3 Computational ADME prediction of benzofuran derivatives 3i and 3m along with the reference compound A-1

Properties	Molecules		
	A-1	3i	3m
(i) Physicochemical			
Molecular weight (g mol ⁻¹)	511.00	322.28	401.17
Consensus log <i>P</i> ^a	4.41	2.34	2.88
log <i>S</i> (ESOL) ^b	-6.41 (poorly soluble)	-4.32 (moderately soluble)	-5.22 (moderately soluble)
(ii) Pharmacokinetics			
GI ^c absorption	High	High	High
BBB ^d permeation	No	No	No
P-gp ^e substrate	No	No	No
(iii) Druglikeness			
Lipinski rule	1 violation: MW ^f > 500	No violation	No violation
Veber rule	No violation	No violation	No violation
Bioavailability score	0.17	0.55	0.55

^a log *P*: lipophilicity. ^b log *S* (ESOL): water solubility, calculated by ESOL method which Quantitative Structure-Property Relationship (QSPR) based model. ^c GI: gastrointestinal. ^d BBB: blood brain barrier. ^e P-gp: permeability glycoprotein. ^f MW: molecular weight.



potential. Indeed, the superior bioavailability score over the reference molecule **A-1** was predicted for these compounds with no violation of Lipinski's criteria in contrary to **A-1**. However, BBB penetration was predicted for compound **3h**. Thus, the benzofuran derivatives **3i** and **3m** seemed to be of further medicinal interest for the discovery and development of new and promising inhibitors of CM.

3. Conclusion

In conclusion, 3-(benzofuran-2-ylmethyl) substituted (pyrazolo/benzo)triazinone derivatives were designed and evaluated *in silico* against CM as potential inhibitors of this enzyme. The docking of target molecules was performed at the interface site of *Mtb*CM (PDB: 2FP2), which is a homodimer, using the open-source tool AutoDock Vina. All the best ranked molecules participated in a strong H-bonding with the ILE67 of B chain at the backbone position in addition to several hydrophobic/van der Waals interactions with the hydrophobic residues. Based on encouraging docking results, the one-pot synthesis of newly designed benzofuran derivatives were carried out using the tandem Pd/Cu-catalyzed Sonogashira cross-coupling followed by intramolecular cyclization of 2-iodophenols with appropriate terminal alkynes. The reaction was carried out in the presence of $(PPh_3)_2PdCl_2$ and CuI in Et_3N at $60\text{ }^\circ\text{C}$ for 2–3 h when a range of novel 3-(benzofuran-2-ylmethyl) substituted (pyrazolo/benzo)triazinone derivatives were obtained in high (>80%) yields. Three molecules *i.e.* **3h**, **3i** and **3m** that participated in good interaction with CM *in silico* showed encouraging (64–65%) inhibition of this enzyme when tested at $30\text{ }\mu\text{M}$ *in vitro*. An SAR within this class of molecules suggested that the inhibitory activity was influenced by the aryl/heteroaryl ring fused with the triazinone moiety and in general the benzotriazinone series emerged as better active molecules than that from pyrazolo-triazinone series. The lower activity observed for compound **3a** and **3d** was reflected by the lack of key H-bond in addition to the lower number of hydrophobic interactions noted for these compounds *in silico*. Considering the molecular docking *in silico*, CM inhibition *in vitro* and computational ADME prediction the benzofuran derivatives **3i** and **3m** were selected as potential hit molecules for further pharmacological studies. Overall, the current efforts not only disclose the Pd/Cu-catalyzed convenient access to novel 3-(benzofuran-2-ylmethyl) substituted (pyrazolo/benzo)triazinone derivatives but also highlight the utility of the related framework for the identification of new inhibitors of CM.

Conflicts of interest

There are no conflicts to declare.

Acknowledgements

SS thanks ICMR, New Delhi, India for a Senior Research Fellowship (TB/41/2020-ECD-I). Authors thank Prof. Gautham G. Shenoy of MAHE, Manipal, Karnataka, India, the

Management of DRILS, Hyderabad, India and Manipal University, Manipal, India for encouragement and support.

Notes and references

- WHO, *Global tuberculosis report 2020*, World Health Organization, Geneva, Switzerland, 2020, ISBN 978-92-4-001313-1.
- For a review, see: M. Khanapur, M. Alvala, M. Prabhakar, K. S. Kumar, R. K. Edwin, P. S. Saranya, R. K. Patel, G. Bulusu, P. Misra and M. Pal, *Bioorg. Med. Chem.*, 2017, **25**, 1725–1736, DOI: [10.1016/j.bmc.2017.02.001](https://doi.org/10.1016/j.bmc.2017.02.001).
- E. Haslam, *Shikimic Acid: Metabolism and Metabolites*, Wiley, New York, 1993.
- End to killer TB? Scientists identify an enzyme that may hold clue*, <https://researchmatters.in/article/end-killer-tb-scientists-identify-enzymemay-hold-clue>.
- G. S. Reddy and M. Pal, *Curr. Med. Chem.*, 2021, **28**, 4531–4568, DOI: [10.2174/092986732766200918144709](https://doi.org/10.2174/092986732766200918144709).
- K. S. Kumar, R. Adepu, S. Sandra, D. Rambabu, G. R. Krishna, C. M. Reddy, P. Misra and M. Pal, *Bioorg. Med. Chem. Lett.*, 2012, **22**, 1146–1150.
- A. Nakhi, B. Prasad, U. Reddy, R. M. Rao, S. Sandra, R. Kapavarapu, D. Rambabu, G. R. Krishna, C. M. Reddy, K. Ravada, P. Misra, J. Iqbal and M. Pal, *Med. Chem. Commun.*, 2011, **2**, 1006–1010.
- G. S. Reddy, A. V. Snehalatha, R. K. Edwin, K. A. Hossain, V. B. Giliyaru, R. C. Hariharapura, G. G. Shenoy, P. Misra and M. Pal, *Bioorg. Chem.*, 2019, **91**, 103155, DOI: [10.1016/j.bioorg.2019.103155](https://doi.org/10.1016/j.bioorg.2019.103155).
- For a review, see: Z. Xu, S. Zhao, Z. Lv, L. Feng, Y. Wang, F. Zhang, L. Bai and J. Deng, *Eur. J. Med. Chem.*, 2019, **162**, 266–276, DOI: [10.1016/j.ejmec.2018.11.025](https://doi.org/10.1016/j.ejmec.2018.11.025).
- V. M. Rao, A. S. Rao, S. S. Rani and M. Junaid, *Int. J. Res. Pharm. Chem.*, 2018, **8**, 112–122, <http://www.ijrpc.com/files/13-01-18/14.pdf>.
- S. D. Gorman, D. S. Winston, D. Sahu and D. D. Boehr, *Biochemistry*, 2020, **59**, 2528–2540.
- P. Prakash, B. Aruna, A. A. Sardesai and S. E. Hasnain, *J. Biol. Chem.*, 2005, **280**, 19641–19648.
- O. Trott and A. J. Olson, *J. Comput. Chem.*, 2010, **31**, 455–461.
- P. Csizmadia, *The Third International Electronic Conference On Synthetic Organic Chemistry*, 1999, September 1–30, p. 367–369.
- R. Huey and G. M. Morris, *Using AutoDock 4 with AutoDockTools: A Tutorial*, The Scripps Research Institute, La Jolla, CA, USA, 2003.
- W. L. DeLano, *CCP4 Newsletter On Protein Crystallography*, 2002, vol. 40, pp. 82–92.
- For a recent review, see: L. Chiummiento, R. D'Orsi, M. Funicello and P. Lupattelli, *Molecules*, 2020, **25**, 2327, DOI: [10.3390/molecules25102327](https://doi.org/10.3390/molecules25102327).
- G. J. S. Doad, J. A. Barltrop, C. M. Pretty and T. C. Owen, *Tetrahedron Lett.*, 1989, **30**, 1597–1598.
- K. Okuro, M. Furuune, M. Enna, M. Miura and M. Nomura, *J. Org. Chem.*, 1993, **58**, 4716–4721.



20 N. G. Kundu, M. Pal, J. S. Mahanty and M. De, *J. Chem. Soc., Perkin Trans.*, 1997, **1**, 2815–2820.

21 J. H. Li, J. L. Li, D. P. Wang, S. F. Pi, Y. X. Xie, M. B. Zhang and X. C. Hu, *J. Org. Chem.*, 2007, **72**, 2053–2057.

22 C. G. Bates, P. Saejueng, J. M. Murphy and D. Venkataraman, *Org. Lett.*, 2002, **4**, 4727–4729.

23 E. A. Jaseer, D. J. C. Prasad and G. Sekar, *Tetrahedron*, 2010, **66**, 2077–2082.

24 W. Zeng, W. Wu, H. Jiang, L. Huang, Y. Sun, Z. Chen and X. Li, *Chem. Commun.*, 2013, **49**, 6611–6613.

25 F. Chahdoura, S. Mallet-Ladeira and M. Gomez, *Org. Chem. Front.*, 2015, **2**, 312–318.

26 A. Ohtaka, T. Teratani, R. Fujii, K. Ikeshita, T. Kawashima, K. Tatsumi, O. Shimomura and R. Nomura, *J. Org. Chem.*, 2011, **76**, 4052–4060.

27 S. Priyadarshini, P. A. Joseph, P. Srinivas, H. Maheswaran, M. L. Kantam and S. Bhargava, *Tetrahedron Lett.*, 2011, **52**, 1615–1618.

28 P. Saejueng, C. G. Bates and D. Venkataraman, *Synthesis*, 2005, **10**, 1706–1712.

29 R. Wang, S. Mo, Y. Lu and Z. Shen, *Adv. Synth. Catal.*, 2011, **353**, 713–718.

30 J. Gil-Moltó and C. Nájera, *Eur. J. Org. Chem.*, 2005, **19**, 4073–4081.

31 R. Cano, M. Yus and D. J. Ramon, *Tetrahedron*, 2012, **68**, 1393–1400.

32 E. K. Yum, O. K. Yang, J. E. Kim and H. J. Park, *Bull. Korean Chem. Soc.*, 2013, **34**, 2645–2649.

33 A. Bruneau, K. P. J. Gustafson, N. Yuan, C. W. Tai, I. Persson, X. Zou and J. E. Bäckvall, *Chem.-Eur. J.*, 2013, **23**, 12886–12891.

34 M. Bhadra, H. S. Sasmal, A. Basu, S. P. Midya, S. Kandambeth, P. Pachfule, E. Balaraman and R. Banerjee, *ACS Appl. Mater. Interfaces*, 2017, **9**, 13785–13792.

35 P. K. Mandali and D. K. Chand, *Synthesis*, 2015, **47**, 1661–1668.

36 (a) L. D. Caspers and B. J. Nachtshei, *Chem.-Asian J.*, 2018, **13**, 1231–1247; (b) B. Panda, *Asian J. Org. Chem.*, 2020, **9**, 492–507; (c) R. Chinchilla and C. Nájera, *Chem. Soc. Rev.*, 2011, **40**, 5084–5121; (d) B. Panda and T. K. Sarkar, *Synthesis*, 2013, **45**, 817–829.

37 (a) N. G. Kundu, M. Pal, J. S. Mahanty and S. K. Dasgupta, *J. Chem. Soc., Chem. Commun.*, 1992, 41–42; (b) M. Pal, V. Subramanian and K. R. Yeleswarapu, *Tetrahedron Lett.*, 2003, **44**, 8221–8225.

38 B. V. D. Rao, S. V. Vardhini, D. Kolli, M. V. B. Rao and M. Pal, *Anti-Cancer Agents Med. Chem.*, 2020, **20**, 580–588, DOI: [10.2174/1871520620666200128120356](https://doi.org/10.2174/1871520620666200128120356), <http://www.eurekaselect.com/178730/article>.

39 R. M. Rao, B. J. Luther, C. S. Rani, N. Suresh, R. Kapavarapu, K. V. L. Parsa, M. V. B. Rao and M. Pal, *Bioorg. Med. Chem. Lett.*, 2014, **24**, 1166–1171.

40 A. Nakhi, M. S. Rahman, G. P. K. Seerapu, R. K. Banote, K. L. Kumar, P. Kulkarni, D. Haldar and M. Pal, *Org. Biomol. Chem.*, 2013, **11**, 4930–4934.

41 D. S. Laxmi, S. V. Vardhini, V. R. Guttikonda, M. V. B. Rao and M. Pal, *Anti-Cancer Agents Med. Chem.*, 2020, **20**, 932–940, DOI: [10.2174/1871520620666200311102304](https://doi.org/10.2174/1871520620666200311102304).

42 S. K. Kim, S. K. Reddy, B. C. Nelson, G. B. Vasquez, A. Davis, A. J. Howard, S. Patterson, G. L. Gilliland, J. E. Ladner and P. T. Reddy, *J. Bacteriol.*, 2006, **188**, 8638–8648.

43 S. Sasso, C. Ramakrishnan, M. Gamper, D. Hilvert and P. Kast, *FEBS J.*, 2005, **272**, 375–389.

44 H. Agrawal, A. Kumar, N. C. Bal, M. I. Siddiqi and A. Arora, *Bioorg. Med. Chem. Lett.*, 2007, **17**, 3053–3058.

45 A. Daina, O. Michielin and V. Zoete, *Sci. Rep.*, 2017, **7**, 1–13.

